NASA TECHNICAL MEMORANDUM 102777

NONLINEAR ANALYSIS AND REDESIGN OF THE MIXED-MODE BENDING DELAMINATION TEST

J. R. Reeder and J. H. Crews, Jr.

January 1991

NASA
National Aeronautics and
Space Administration

Langley Research Center
Hampton, Virginia 23665-5225

SUMMARY

The Mixed-Mode Bending (MMB) test uses a lever to simultaneously apply mode I and mode II loading to a split-beam specimen. An iterative analysis that accounts for the geometric nonlinearity of the MMB test was developed. The analysis accurately predicted the measured load-displacement response and the strain energy release rate, G, of an MMB test specimen made of APC2 (AS4/PEEK). The errors in G when calculated using linear theory were found to be as large as 30% in some cases. Because it would be inconvenient to use a nonlinear analysis to analyze MMB data, the MMB apparatus was redesigned to minimize the nonlinearity. The nonlinear analysis was used as a guide in redesigning the MMB apparatus. With the redesigned apparatus, loads are applied through a roller attached to the lever and loaded just above the midplane of the test specimen. The redesigned MMB apparatus has geometric nonlinearity errors of less than 3%, even for materials substantially tougher than APC2. This apparatus was demonstrated by measuring the mixed-mode delamination fracture toughness of APC2. The data from the redesigned MMB apparatus were analyzed with a linear analysis which yielded results similar to those found with the original apparatus and the nonlinear analysis.

INTRODUCTION

Delamination continues to be one of the major problems limiting the use of composite materials in primary structures. A major step toward predicting delamination is characterizing a material's delamination fracture toughness. Delamination fracture toughness is often expressed in terms of the critical strain energy release rate, G_c, corresponding to delamination growth.

Many tests have been used to measure fracture toughness. The double cantilever beam (DCB) test[1] is most often used to measure mode I (opening) delamination fracture toughness. The end-notched flexure (ENF) test[2] is most often used to measure mode II (sliding shear) delamination fracture toughness. However, delamination in structures is usually not a result of pure mode I or pure mode II loading, so it is important that the delamination fracture toughness be known for mixed-mode loading.

Several tests have been used for measuring mixed-mode fracture toughness in the mode I/mode II range. These tests include: the edge-delamination tension[3], the crack-lap shear[4], the Arcan[5], the asymmetric double cantilever beam[6], the mixed-mode flexure[7], and the variable mixed-mode[8] test. However, all of these tests have one or more problems which limit their usefulness. The mixed-mode bending (MMB) test[9] seems to solve many of these problems. The MMB test uses a lever to simultaneously apply DCB and ENF type loadings, and by varying the lever length, practically any mode I/mode II ratio can be obtained. In addition, the MMB test can be analyzed using simple beam theory equations developed for the DCB and ENF tests, and this analysis can be used to separate the mode I and mode II components. Furthermore, delamination growth is stable for most MMB test configurations and the mixed-mode ratio stays essentially constant during delamination growth. However, when the MMB test was used with a tough

material such as APC2 (AS4/PEEK), rather large displacements were observed. These large displacements caused geometric nonlinearities. The purpose of this paper is to analyze the geometric nonlinearities of the MMB test and to introduce a redesigned MMB test apparatus that minimizes these nonlinearities.

An analysis was developed to account for the geometric nonlinearity of the MMB loading apparatus and throughout this paper the term nonlinearity will refer to geometric nonlinearity. The analysis was used to calculate the load-displacement response of MMB tests as well as the strain energy release rates. Since it would be inconvenient to use a nonlinear analysis to analyze MMB data, the MMB apparatus was redesigned to reduce the nonlinearity. The nonlinear analysis was used to optimize the redesigned MMB apparatus. This redesigned apparatus was demonstrated by measuring the fracture toughness of APC2. The results are compared to a previous study which used the original apparatus.

LIST OF SYMBOLS

a	Delamination length
b	Specimen width
c	Lever length
E_{11}	Longitudinal modulus
E_{22}	Transverse modulus
G	Strain energy release rate
G_T	Total strain energy release rate
G_{12}	Shear modulus
h	Specimen half-thickness
I	Bending moment of inertia of specimen half-thickness
L	Specimen half-span length
M	Moment at delamination tip
M_A, M_B	Moment at the delamination tip due to loading at points A and B, respectively.

P	Load at a point
P_a	Applied load
v	Load-point height above specimen midplane
x,y	Coordinates in specimen reference system
X,Y	Global coordinates
δ	Load-point displacement
λ	Elastic foundation parameter
ϕ	Rotation of specimen cross section at a point
θ_O	Rotation of specimen coordinate system
θ_L	Rotation of lever

Superscripts

A,B,C,D,F	Value at points A, B, C, D, and F on the MMB apparatus
i	Refers to the ith iteration

Subscripts

c	Fracture toughness (critical strain energy release rate)
lin	Value calculated using linear theory
nl	Value calculated using nonlinear analysis
x,y,X,Y	Value in the x, y, X, and Y direction, respectively
I, II	Mode I and Mode I component, respectively

MMB TEST PROCEDURE

The MMB apparatus used in previous studies is shown in figure 1. Load is applied to a split-beam specimen by means of a lever where the distance, c, between the load-point and the fulcrum can be varied. The mode I and mode II loadings are applied simultaneously to the split-beam specimen using this lever. The downward load applied at the fulcrum of the lever produces a mode II loading similar to the ENF test. The upward load at the end of the lever creates a mode I loading similar to the DCB test. By changing loading point on the lever, and therefore the length c, the ratio of mode I to mode II loading can be changed. Load points were chosen to produce G_I/G_{II} ratios of 4/1, 1/1,

and 1/4. Tests were also conducted under pure mode II where the lever was loaded directly above the center roller resulting in 3 point bending and under pure mode I where the lever was removed and the top hinge was pulled upward as in the DCB test.

The material used in this study was APC2, a tough thermoplastic composite made of AS4 fibers in a PEEK (polyetheretherketone) matrix. The longitudinal modulus, E_{11}, was measured in flexure to be 18.7 Msi using a 3-point bend test with a 3 in. span length. The transverse modulus, E_{22}, and shear modulus, G_{12}, were found from the literature to be 1.46 Msi and 0.8 Msi, respectively[9].

Unidirectional 24-ply test specimens were produced from two 6"x12" panels. The specimen length was 6 in.; the width, b, was 1 in.; and the nominal thickness, h, was 0.12 in. Each specimen contained a 0.5 mil thick Kapton delamination starter which was 2.5 in. long and placed at one end of the specimen between the 12th and 13th plies. Hinges were bonded to the specimen as shown in figure 1 so that the initial delamination length, a, was 1 in. The half-span length, L, of each test was 2 in.

Each specimen was precracked using a 4/1 mixed-mode ratio loading to a delamination length of approximately 1.25 inches to be consistent with previous tests[9]. Each specimen was then reloaded to produce delamination growth under one of the mixed-mode or pure-mode conditions. The specimens were loaded in displacement control at a rate of 0.05 in/min at the lever loading point. The maximum load was used as the critical load in the calculation of fracture toughness, G_c. The delamination length, a, which was determined during the test by observing the edge of the specimen through a 7x microscope, was also used in the calculation of G_c. The edge of the specimen was coated

with a white, water soluble typewriter correction fluid to increase the visibility of the delamination.

The load-displacement response was measured during each fracture toughness test. The displacement measurements were taken from the crosshead position but were then corrected for the compliance of the load frame and the MMB apparatus. This compliance was measured using an extremely stiff specimen (3/8 inch steel) in the test apparatus. This linear correction to the displacement measurements was less than 6%. A second correction was made to the displacement measurements to correct for a small initial nonlinearity. This nonlinearity, which is believed to be caused by specimen seating, was corrected by subtracting a small constant displacement (less than 2% of the maximum displacement).

SOURCES OF NONLINEARITY

In reference 9, a finite element analysis, and a modified beam theory analysis, were shown to predict the load-displacement curve of the MMB test quite well at low load levels where the curve is linear. However, at higher loads required when testing tough materials such as APC2, there is some nonlinearity evident in the load-displacement curves before delamination onset. This nonlinearity can be seen in figure 2, which shows a load-displacement curve for an MMB test on an APC2 specimen with a 1/1 mixed-mode ratio. The dimensions of the specimen were chosen so that specimen nonlinearity would be negligible for either the DCB[10] or ENF[11] tests. Since the MMB test is simply a combination of these tests, the specimen nonlinearity is small in this case as well. Similarly, since material nonlinearity was not observed in the pure mode tests, it should not be present in the MMB test. Therefore, most of this nonlinearity is believed to be caused by geometric nonlinearity of the

loading apparatus alone. The APC2 specimen had a nonlinear responce when loaded in the original MMB apparatus primarily because the loading on the apparatus changed direction as the specimen deformed. The lever was loaded by a roller, and when the lever rotated as the system was loaded, the loading direction changed so that it was always perpendicular to the lever as seen in figure 1(b).

ANALYSIS

To understand the effects of the geometric nonlinearity, a nonlinear analysis was developed. This analysis was used to calculate the strain energy release rate and the displacement of the MMB test apparatus accounting for the nonlinearity of the apparatus. The analysis was also helpful in understanding more fully the causes of the nonlinearity. As a result, the analysis was used to optimize a redesigned MMB apparatus which reduces the nonlinearity of the test.

The nonlinear analysis uses an iterative approach described by the flow chart in figure 3. The analysis is also explained in detail in the appendix. The first step in this analysis is to choose an applied load, P_a, and apply it to the initial position of the lever. To calculate fracture toughness, this applied load will be the critical load measured during an MMB test. This loading is then used to calculate the initial loading which would exist on the undeformed specimen. This specimen loading is used with linear beam theory to calculate the deformed shape of the specimen. The deformation of the specimen causes the lever to rotate and displace and its new position is calculated. The rotation of the lever causes a horizontal component of applied load to develop due to the roller loading which always bears perpendicular to the lever surface. The loading on the specimen is recalculated using the new lever loading and

position. The next iteration is begun by recalculating the deformed shaped of the specimen from the specimen loading. The iterative process is repeated until the change in the lever rotation from one iteration to the next is negligible. Once the analysis converges, the mode I and mode II strain energy release rate can be calculated from the loading on the specimen. Because of the iterative nature of this analysis, a computer program was created to perform the calculations.

The mode I and mode II components of G for split-beam specimens have been related to the moments applied to the crack tip region[12]. For a specimen with arms of equal thickness, the G equations presented in reference 12 reduce to

$$(G_I)_{nl} = \frac{M_I^2}{bE_{11}I} \tag{1}$$

$$(G_{II})_{nl} = \frac{3M_{II}^2}{4bE_{11}I} \tag{2}$$

where M_I and M_{II} are the moments symmetrically and antisymmetrically applied to the two arms of the split-beam specimen, respectively. In the present study, these moments are calculated using the nonlinear analysis described in the appendix and correspond to mode I and mode II loading.

The G equations were modified[9] to account for rotations about the crack tip[13] and shear deformation[11,14] as has been done for the pure mode tests.

$$(G_I)_{nl} = \frac{M_I^2}{bE_{11}I}\left(1 + \frac{2}{\lambda a} + \frac{1}{(\lambda a)^2}\right) + \frac{6(P_I)^2}{5b^2G_{12}h} \tag{3}$$

$$(G_{II})_{nl} = \frac{3M_{II}^2}{4bE_{11}I} + \frac{9(P_{II})^2}{80b^2G_{12}h} \qquad (4)$$

where $\lambda = \frac{1}{h}\sqrt[4]{\frac{6E_{22}}{E_{11}}}$

The terms P_I and P_{II} correspond to the loading that would be applied to the specimen to obtain a pure mode I (DCB) or a pure mode II (ENF) test. The calculation of these terms is described in the appendix.

The linear analysis developed in reference 9 is used to compare with the nonlinear analysis. This analysis assumes that there is no change in loading due to specimen deformation, and the calculation of G is therefore much simpler.

$$(G_I)_{lin} = \frac{4P_a^2(3c-L)^2}{64bL^2E_{11}I}\left[a^2 + \frac{2a}{\lambda} + \frac{1}{\lambda^2} + \frac{h^2E_{11}}{10G_{12}}\right] \qquad (5)$$

$$(G_{II})_{lin} = \frac{3P_a^2(c+L)^2}{64bL^2E_{11}I}\left[a^2 + \frac{h^2E_{11}}{5G_{12}}\right] \qquad (6)$$

ANALYSIS RESULTS

The nonlinear analysis was evaluated by comparing calculated and measured load-displacement curves. Next, the analysis was used to investigate the effect of the nonlinearity on G. The errors due to ignoring the nonlinearity were calculated. The MMB apparatus was redesigned to minimize the nonlinearity.

Figure 4 shows measured load-displacement curves compared to the calculated curves from the linear beam theory analysis and the nonlinear analysis. There is nonlinearity throughout the mixed-mode range studied. The nonlinearity is much more pronounced where there is a substantial mode II component. The nonlinear analysis accurately predicts the load displacement response of the MMB test up to load levels where the delamination would begin to extend.

The excellent agreement of the analysis calculations with measured displacements indicates that the analysis should also accurately calculate the strain energy release rate of the MMB specimen. However, it is much simpler to determine G with the linear analysis than with the nonlinear analysis. The error in G caused by ignoring the nonlinearity was examined. First, the load required to extend a delamination was calculated for a material with a G_c of 10 in-lb/in^2. This value was chosen to represent a material such as APC2. This calculated critical load was used to calculate the mode I and mode II strain energy release rates using both linear and nonlinear analyses. The results of the two analyses were compared to determine the errors due to nonlinearity. These errors were calculated using the following equations.

$$G_I \text{ Error} = \frac{(G_I)_{lin} - (G_I)_{nl}}{(G_T)_{nl}} \times 100 \qquad (7)$$

$$G_{II} \text{ Error} = \frac{(G_{II})_{lin} - (G_{II})_{nl}}{(G_T)_{nl}} \times 100 \qquad (8)$$

Notice that the errors in equations 7 and 8 are expressed as a percentage of the total strain energy release rate, $(G_T)_{nl}$, where $(G_T)_{nl} = (G_I)_{nl} + (G_{II})_{nl}$. Figure 5

shows these nonlinearity errors versus delamination length. The errors in calculating G could be as large as 30% which is unacceptable.

As previously mentioned, the nonlinearity was primarily due to the change in the direction of the applied lever load. The applied load, which was initially vertical, developed a horizontal component as the lever rotated as seen in figure 1. This horizontal force created a substantial moment about the upper hinge pin because the lever was 2.9 inches above the specimen mid-plane. Since the moment caused by the horizontal load is in the opposite direction to the moment created by the vertical applied load, it causes a reduction in G. The G calculated using the linear analysis is erroneously high because it does not account for this horizontal lever load. The effect of the moment is much more pronounced for the mode I component, thus causing the mode I error to be larger than the mode II error for each mixed-mode case as shown in figure 5. The largest error is for the 1/1 mixed-mode ratio.

REDESIGN OF THE MMB APPARATUS

Because it would be inconvenient to use a nonlinear analysis to analyze MMB data, the MMB apparatus was redesigned to minimize the nonlinearity so that a linear analysis could be used. The obvious solution to the nonlinearity problem is to eliminate the horizontal force which develops on the lever as it rotates. The horizontal force can be eliminated by simply attaching the roller to the lever and loading the roller with a horizontal surface attached to the load machine. Since the surface on which the roller bears no longer rotates, the reaction on the lever will remain vertical.

However, when the roller is attached to the lever, it moves horizontally as the lever rotates about the hinge pin. This causes the horizontal distance from the hinge to change, as shown by Δc in figure 6(a). The changing load location

changes the moment about the hinge pin, causing a geometric nonlinearity. This effect is reduced as the height of the roller above the specimen midplane is reduced, as shown in figure 6(b). Figure 7 shows how the errors due to this nonlinearity change with roller height. At a load-point height, v, of 0.6 inches the nonlinearity error is approximately ±2%. Therefore, with this redesigned MMB apparatus, a linear analysis can be used to analyze the test data and the nonlinearity error will be small. These results were calculated for a toughness of G_c=10 in-lb/in^2 with the graphite/PEEK test specimen described earlier. The results are also valid for tests on other materials such as glass/epoxy having a different modulus, provided the specimens have a comparable bending stiffness ($E_{11}I$).

The design of the test fixture, with the roller attached to the lever at a load-point height of 0.6 inches, required a saddle-like device so that the lever did not contact the specimen during loading. The saddle extends down on both sides of the lever and the test specimen, as shown in figure 8. The saddle holds one bearing on each side of the lever such that the top of the bearing is at 0.6 inches above the mid-plane of the specimen. The apparatus is loaded with a yoke which contacts the rollers without touching the lever. To change the lever length and therefore the mixed-mode ratio, the saddle can be moved on the lever.

Figure 9 shows load-displacement curves measured with the redesigned apparatus when the lever lengths were set to produce the 4/1, 1/1, and 1/4 mixed-mode conditions. These experimentally measured curves agree closely with the linear analysis calculations. The redesigned MMB apparatus has significantly less nonlinearity.

The reduction in nonlinearity can also be seen in figure 10 where percent error in G from equations 7 and 8 is plotted versus delamination length. From

this figure, it can be seen that for a material as tough as APC2 the error is less than $\pm$ 3% as the delamination grows over the test region.

The errors due to nonlinearity with a graphite reinforced composite specimen having a 1.75 in. delamination length loaded by the redesigned MMB apparatus are plotted versus delamination fracture toughness in figure 11. The figure shows that nonlinearity error will be less than about $\pm$3% for materials with G_c as high as 20 in-lb/in^2. Therefore, the nonlinearity errors will be acceptably small even for materials twice as tough as APC2 provided the bending stiffness of the specimens is comparable to that used in this study.

EXPERIMENTAL RESULTS

The APC2 toughness testing in reference 9 was conducted with the original MMB apparatus and a linear analysis. Results from reference 9 are shown as open circles in figure 12. These data points are slightly different from those presented in reference 9 because the critical load was redefined to be the maximum load from the load-displacement curve instead of the load where the slope changes abruptly. Only minor shifts in the data resulted and the data are now comparable to those from the present study. The results from reference 9 were also reanalyzed using the nonlinear analysis and are shown as filled circles and by the dashed line in figure 12. Notice that the G_I/G_{II} ratios have changed and that all the G values calculated using the nonlinear analysis are lower than the linear values. These differences should be expected from the errors presented in figure 5. Notice that the effects of nonlinearity are most pronounced on the mode I component in the middle of the mixed-mode range, as discussed earlier.

The mixed-mode fracture toughness of APC2 was also measured with the redesigned apparatus. A typical load-displacement curve from one of these tests is shown in figure 13. The curve is nearly linear up to the region near the maximum load point. The deviation from linearity in this region is believed due to damage occurring at the delamination tip and not to apparatus nonlinearities. The maximum load was used as the critical value in calculating fracture toughness which is consistent with the results from the previous study.

The toughness measurements made with the redesigned apparatus and the linear analysis are presented in figure 12 as open squares and a dash-dot line. These results should agree with the data from the previous study, but as shown in this figure, the redesigned data (dash-dot line) lie below those from the original apparatus (dashed line). This discrepancy is believed to be due to material differences. Note that the average G_{Ic} changed from 7.2 in-lb/in^2 for the previous study to 5.5 in-lb/in^2 for the present study even though the mode I, DCB test and the analysis were identical for the two studies. Furthermore, the flexural modulus changed from 16.8 Msi for the previous study to 18.7 Msi in the present study. Since G_{Ic} and G_{IIc} are inversely related to the modulus as seen in equations 5 and 6, this change in modulus may also contribute to the discrepancy in toughness between the two studies. These material differences can probably be attributed to processing[15,16]. Since the data from both studies can be modeled with straight lines that have similar slopes, the fracture toughness measurements from the redesigned MMB apparatus and a simple linear analysis are believed to be accurate. The linear curve fit agrees with the following failure criterion suggested in references 17 and 18.

$$\frac{G_I}{G_{Ic}} + \frac{G_{II}}{G_{IIc}} = 1 \qquad (9)$$

CONCLUDING REMARKS

The MMB test uses a lever to simultaneously apply mode I and mode II loading to a split-beam specimen. Rotations of the lever were found to produce geometric nonlinearities in the load displacement response of the MMB apparatus. An analysis of these geometric nonlinearities accurately predicted the load-displacement response of the apparatus. The analysis showed that the nonlinearity had a large effect on the measured delamination fracture toughness of tough materials calculated using linear beam theory.

The MMB loading apparatus was redesigned to virtually eliminate the nonlinearities. A complex nonlinear analysis is therefore no longer needed to analyze MMB data. The analysis showed that an optimum design is achieved when the MMB loading was applied through a roller which is attached to the lever so that the roller contact height is 0.6 inches above the specimen mid-plane. With the redesigned loading apparatus, the errors due to the nonlinearity are less than $\pm$ 3% for the APC2 specimen used in this study, and hence, can be ignored. Similarly small errors should be expected for other materials provided the specimen bending stiffness is comparable to that used in the present study.

The delamination fracture toughness of APC2, was measured with the redesigned apparatus and compared to results found earlier using the original apparatus. After the previous data were reanalyzed using the nonlinear analysis, they were similar to the data from the redesigned MMB apparatus analyzed with the linear analysis. The difference in toughness between the previous study and the present study was attributed to manufacturing differences in the material. Therefore, using the redesigned MMB apparatus,

delamination fracture toughness can be calculated from test data using a simple linear beam theory analysis.

REFERENCES

1. Wilkins, D. J.; Eisenmann, J. R.; Camin, R. A.; Margolis, W. S.; Benson, R. A.: "Characterizing Delamination Growth in Graphite-Epoxy," Damage in Composite Materials, ASTM STP 775, K. L. Reifsnider, Ed., American Society for Testing and Materials, Philadelphia, 1982, pp. 168-183.

2. Russell , A. J.: "On the Measurement of Mode II Interlaminar Fracture Energies," DREP Materials Report. 82-0, Defence Research Establishment Pacific, Victoria, December, 1982.

3. O'Brien, T. K.: "Mixed-Mode Strain-Energy-Release Rate Effects on Edge Delamination of Composites," Effects of Defects in Composite Materials, ASTM STP 836, D. J. Wilkins, Ed., American Society for Testing and Materials, Philadelphia, 1984, pp. 125-142.

4. Johnson, W. S.: "Stress Analysis of the Crack-Lap-Shear Specimen: An ASTM Round-Robin," Journal of Testing and Evaluation, JTEVA, Vol. 15, No. 6, November 1987, pp. 303-324.

5. Arcan, M.; Hashin, Z.; and Voloshin, A.: "A Method to Produce Uniform Plane-Stress States with Applications to Fiber-Reinforced Materials," Experimental Mechanics, Vol. 28, April 1978, pp. 141-146.

6. Bradley, W. L.; and Cohen, R. N.: "Matrix Deformation and Fracture in Graphite-Reinforced Epoxies," Delamination and Debonding of

Materials, ASTM STP 876, W. S. Johnson, Ed., American Society for Testing and Materials, Philadelphia, 1985, pp. 389-410.

7. Russell, A. J.; and Street, K. N.: "Moisture and Temperature Effects on the Mixed-Mode Delamination Fracture of Unidirectional Graphite/Epoxy," Delamination and Debonding of Materials, ASTM STP 876, W. S. Johnson, Ed., American Society for Testing and Materials, Philadelphia, 1985, pp. 349-370.

8. Hashemi, S.; Kinloch, A. J.; and Williams J. G.: "Interlaminar Fracture of Composite Materials," 6th ICCM & 2nd ECCM Conference Proceedings, Vol. 3, London, July 1987, pp. 3.254-3.264.

9. Reeder, J. R.; and Crews, J. H., Jr.: "The Mixed-Mode Bending Method for Delamination Testing," AIAA Journal, Vol. 28, No. 7, July 1990, pp. 1270-1276.

10. Naik, R. A.; Crews, J. H., Jr.; and Shivakumar, K. N.: "Effects of T-Tabs and Large Deflections in DCB Specimen Tests," NASA TM 101677; November 1989. (to be published in ASTM STP 1110)

11. Carlsson, L. A.; Gillespie, J. W., Jr.; and Pipes, R. B.: "On the Analysis and Design of the End Notched Flexure (ENF) Specimen for Mode II Testing," Journal of Composite Materials, Vol. 20, November 1986, pp. 594-604.

12. Williams, J. G.: "On the Calculation of Energy Release Rates For Cracked Laminates," International Journal of Fracture; Vol. 36, February 1988, pp. 101-119.

13. Kanninen, M. F.: "An Augmented Double Cantilever Beam Mode I for Studying Crack Propagation and Arrest," International Journal of Fracture, Vol. 9, No. 1, March 1973, pp. 83-92.

14. Aliyu, A. A.; and Daniel, I. M.: "Effects of Strain Rate on Delamination Fracture Toughness of Graphite/Epoxy," Delamination and Debonding of Materials, ASTM STP 876, W. S. Johnson, Ed., American Society of Testing and Materials, Philadelphia, 1985, pp. 336-348.

15. Curtis, P. T.; Davies, P.; Partridge, I. K.; and Sainty, J. P.: "Cooling Rate Effects in PEEK and Carbon Fibre-PEEK Composites," 6th ICCM & 2nd ECCM Conference Proceedings, Vol. 4, London, July 1987, pp. 4.401-4.412.

16. Jar, P. Y.; Davies, P.; Cantwell, W.; Schwartz, C.; Grenestedt, J.; and Kausch, H. H.: "Manufacturing Engineering Components with Carbon Fibre Reinforced PEEK," Developments in the Science and Technology of Composite Materials, 4th ECCM Conference Proceedings, New York, September 1990, pp. 819-824.

17. Jurf, R. A.; and Pipes, R. B.: "Interlaminar Fracture of Composite Materials," Journal of Composite Materials, Vol. 16, September 1982, pp. 386-394.

18. Johnson, W. S.; and Mangalgiri, P. D.: "Influence on the Resin on Interlaminar Mixed-Mode Fracture," Toughened Composites, ASTM STP 937, Norman J. Johnston, Ed., American Society for Testing and Materials, Philadelphia, PA, 1987, pp. 295-315.

APPENDIX A

NONLINEAR ANALYSIS OF MMB APPARATUS

To determine the effect of the geometric nonlinear response of the MMB apparatus, a nonlinear analysis was developed. This analysis was first developed for the original MMB apparatus and then extended to the redesigned MMB apparatus. The analysis uses an iterative approach to calculate the displacement and strain energy release rate of the MMB specimen accounting for the change in loading due to the apparatus deflection. The procedure used in this analysis is outlined by the flow chart in figure 3. In this procedure, first the initial loading on the lever and specimen are calculated. With this loading, the deformation of the specimen is found using linear beam theory. The deformation of the specimen causes the lever to rotate. With the original MMB apparatus, the lever was loaded by a roller so the applied force was always normal to the lever. Therefore as the lever rotated, a horizontal component of force developed on the lever as seen in figure 1(b). The new position of the lever is therefore calculated from the specimen deformation so that the loading on the lever can be determined. The new lever loading is then used to recalculate the loading on the test specimen. At this point, the convergence of the solution is checked. If the rotation of the lever has changed significantly since the last iteration, then the next iteration is begun by calculating the specimen deformation from the loading on the specimen. If the rotation of the lever has not changed significantly, then the solution has converged and the loading is used to calculate the mode I and mode II strain energy release rates. This appendix first describes in detail how each step of the analysis was

performed for the original MMB apparatus and then briefly describes how the analysis was extended to the redesigned MMB apparatus.

Original MMB Apparatus

Initial loading.- Initially the lever is horizontal and the applied loading P_a on the beam is therefore vertical and directed downward. Since the specimen is initially undeformed, the loading on the specimen shown in figure A1(a) can be calculated.

$$\begin{aligned} P_y^A &= P_a\left(\frac{c}{L}\right) \\ P_y^B &= P_a\left(\frac{L-c}{2L}\right) \\ P_y^C &= -P_a\left(\frac{c+L}{L}\right) \\ P_y^D &= P_a\left(\frac{L+c}{2L}\right) \\ P_x^A &= P_x^B = P_x^C = P_x^D = 0 \end{aligned} \tag{A1}$$

The superscripts on load, P, indicate points on the specimen and the subscripts indicate the component of load. A mode I load, P_I, and a mode II load, P_{II}, are also calculated. These loads are used in corrections to linear beam theory which were developed for the mode I, DCB test and the mode II, ENF test, respectively.

$$\begin{aligned} P_I &= \frac{P_y^A - P_y^B}{2} \\ P_{II} &= -P_y^C \end{aligned} \tag{A2}$$

Specimen deformation.- The specimen deformation, calculated using linear beam theory, is expressed in terms of a coordinate system at the

delamination tip (point O). This coordinate system was chosen because it simplifies the description of the specimen deformation. This specimen coordinate system (x,y) moves and rotates with respect to the global coordinate system (X,Y) which will be described later. For each point of interest, the vertical and horizontal location as well as the slope of the deformed beam (Y, X, and ϕ, respectively) are calculated using equations A3. Here, the simple beam theory deformation has been corrected for shear deformation[11,14] and displacement due to rotation at the delamination tip[13]. The rotation at the delamination tip is found using a beam on an elastic foundation correction. This correction is similar to that used with the DCB test and the mode II loading is used in this correction. The points of interest on the beam are not located at the specimen midplane so the vertical locations were corrected for this initial offset. Points A and B are located at the center of the bonded hinge pin and points C and D are located at the specimen surface. The axial displacements of the specimen are small and therefore neglected, so the only corrections made to the horizontal locations are for the rotation of the specimen cross section when the additional height of the hinge, h^*, might make this correction significant.

Beam Theory	Elastic Foundation and Shear Correction	Hinge Height and Beam Thickness Corrections
$y^A = \frac{P_y^A a^3}{3E_{11}I}$	$+ \frac{P_I a^3}{3E_{11}I}\left(\frac{3}{\lambda a} + \frac{3}{(\lambda a)^2}\right) + \frac{12P_y^A a}{10bhG_{12}}$	$+h+h^*$
$x^A = a$		$-\phi^A\left(\frac{h}{2}+h^*\right)$
$\phi^A = \frac{P_y^A a^2}{2E_{11}I}$	$+ \frac{P_I a^2}{3E_{11}I}\left(\frac{3}{\lambda a} + \frac{3}{(\lambda a)^2}\right) + \frac{12P_y^A}{10bhG_{12}}$	
$y^B = \frac{P_y^B a^3}{3E_{11}I}$	$+ \frac{P_I a^3}{3E_{11}I}\left(\frac{3}{\lambda a} + \frac{3}{(\lambda a)^2}\right) + \frac{12P_y^B a}{10bhG_{12}}$	$-(h+h^*)$
$x^B = a$		$+\phi^B\left(\frac{h}{2}+h^*\right)$
$\phi^B = \frac{P_y^B a^2}{2E_{11}I}$	$+ \frac{P_I a^2}{3E_{11}I}\left(\frac{3}{\lambda a} + \frac{3}{(\lambda a)^2}\right) + \frac{12P_y^B}{10bhG_{12}}$	(A3)
$y^C = \frac{P_y^C(L-a)^3}{24E_{11}I} + \frac{P_y^D(L-a)^2(5L-2a)}{48E_{11}I}$	$+ \frac{12\left(P_y^C + P_y^D\right)(L-a)}{20bhG_{12}}$	$+h$
$x^C = a - L$		
$\phi^C = \frac{-P_y^C(L-a)^2}{16E_{11}I} - \frac{P_y^D(L-a)(3L-a)}{16E_{11}I}$	$- \frac{12\left(P_y^C + P_y^D\right)}{20bhG_{12}}$	
$y^D = \frac{P_y^C(L-a)^2(5L-2a)}{48E_{11}I} + \frac{P_y^D(2L-a)^3}{24E_{11}I}$	$+ \frac{12P_y^D(2L-a)}{20bhG_{12}} + \frac{12P_y^C(L-a)}{20bhG_{12}}$	$-h$
$x^D = a - 2L$		
$\phi^D = \frac{-P_y^C(L-a)^2}{16E_{11}I} - \frac{P_y^D(2L-a)^2}{16E_{11}I}$	$- \frac{12P_y^D}{20bhG_{12}}$	

where $\lambda = \frac{1}{h}\sqrt[4]{\frac{6E_{22}}{E_{11}}}$

Lever position and loading.- The loading on the lever changed as the specimen deforms and caused the lever position to change. The position of the lever must be determined relative to the load frame. Therefore, a global coordinate system (X,Y) is set up which is located at point B as shown on in figure A1(b). The angle between the specimen coordinate system and the global system is θ_O.

$$\theta_O = -\tan^{-1}\left(\frac{y^B + h^* - y^D}{2L}\right) \tag{A4}$$

This was calculated by rotating the deformed shape of the specimen so that its left end (point D) remains in contact with the roller, as shown in figure A1. The location of the specimen coordinate system is described by locating its origin, point O, in the global reference system.

$$\begin{aligned} X^O &= -x^B\cos\theta_O + y^B\sin\theta_O \\ Y^O &= -x^B\sin\theta_O - y^B\cos\theta_O \end{aligned} \tag{A5}$$

The angle of the lever, θ_L, with respect to the global reference system is calculated by rotating the lever so that the center roller remains in contact with the specimen surface.

$$\theta_L = \theta_O + \tan^{-1}\left(\frac{y^A - h^* - y^C}{L}\right) \tag{A6}$$

To determine the location of the load point, the location of point A where the lever is attached to the beam must be determined in the global system.

$$X^A = (x^A - x^B)\cos\theta_O - (y^A - y^B)\sin\theta_O$$
$$Y^A = (x^A - x^B)\sin\theta_O + (y^A - y^B)\cos\theta_O \qquad \text{(A7)}$$

The location of the load point F does not change in the X direction. The vertical location is found from the displacement at point A plus the rotation of the lever.

$$X^F = -(L + c)$$
$$Y^F = Y^A + (v - h - h^*)\cos\theta_L - \left(X^A - X^F - (v - h - h^*)\sin\theta_L\right)\tan\theta_L \qquad \text{(A8)}$$

The displacement measured during an MMB test corresponds to the change in the vertical displacement of point F.

$$\delta = v + h + h^* - Y^F \qquad \text{(A9)}$$

The loading on the lever is calculated using equations A10. The first equation results since the test machine only measures the vertical component of load and it was applied in the negative Y direction. The second equation results because the load was applied through a roller and therefore, was always perpendicular to the lever surface.

$$P_Y^F = -P_a$$
$$P_X^F = -P_Y^F \tan\theta_L \qquad \text{(A10)}$$

Recalculate specimen loading.- To calculate the loading on the specimen, the loads applied to the lever and the location of point F must be determined in the specimen coordinate system.

$$
\begin{aligned}
x^F &= (X^F - X^O)\cos\theta_O + (Y^F - Y^O)\sin\theta_O \\
y^F &= -(X^F - X^O)\sin\theta_O + (Y^F - Y^O)\cos\theta_O \\
P_x^F &= P_X^F\cos\theta_O + P_Y^F\sin\theta_O \\
P_y^F &= -P_X^F\sin\theta_O + P_Y^F\cos\theta_O
\end{aligned}
\tag{A11}
$$

These applied loads are equilibrated by reactions at the roller and the hinge, points C and A, respectively. The loads applied to the specimen are equal and opposite to the reactions on the lever. The loading at point C was through a roller so it was always perpendicular to the specimen surface.

$$
\begin{aligned}
P_y^C &= \frac{P_y^F(x^F - x^A) - P_x^F(y^F - y^A)}{(x^C - x^A) + \phi^C(y^C - y^A)} \\
P_x^C &= -\phi^C P_y^C \\
P_y^A &= P_y^F - P_y^C \\
P_x^A &= P_x^F - P_x^C
\end{aligned}
\tag{A12}
$$

The loading at points C and A are equilibrated by reactions at points B and D. The reaction at point D is also through a roller so it will be perpendicular to the specimen surface.

$$
\begin{aligned}
P_y^D &= \frac{-P_y^C(x^C - x^B) + P_x^C(y^C - y^B) - P_y^A(x^A - x^B) + P_x^A(y^A - y^B)}{(x^D - x^B) + \phi^D(y^D - y^B)} \\
P_x^D &= -\phi^D P_y^D \\
P_y^B &= -P_y^D - P_y^C - P_y^A \\
P_x^B &= -P_x^D - P_x^C - P_x^A
\end{aligned}
\tag{A13}
$$

The mode I and mode II loading should be recalculated at this point using the recalculated specimen loads and equation A2.

Convergence Test.- The specimen loads are used in the next iteration to calculate specimen deformation and therefore new specimen loads. This iterative process is continued until it converges. The test for convergence is based on the rotation of the lever.

$$\theta_L^i - \theta_L^{i-1} \le 0.000001 \qquad \text{(A14)}$$

where i indicates the present iteration and i-1 indicates the previous iteration. Once the lever rotation has converged, the G from the nonlinear analysis can be calculated using the converged values of load and position. Also, the converged value of displacement along with the chosen load, P_a, can be used as the a point on a load-displacement curve for the split beam specimen in the MMB apparatus. To create a load-displacement curve, many values of P_a are used in this analysis.

Strain energy release rate.-The G of a split-beam type specimen can be related to the moments at the delamination tip. The moments at the delamination tip in the top half of the split-beam specimen, M_A, is due to the specimen loading at point A. Similarly, the moment in the bottom half of the beam, M_B, is due to loading at point B.

$$\begin{aligned} M_A &= P_y^A x^A - P_x^A y^A \\ M_B &= P_y^B x^B - P_x^B y^B \end{aligned} \qquad \text{(A15)}$$

These moments can be divided into their symmetric (mode I) and antisymmetric (mode II) components.

$$\begin{aligned} M_I &= \frac{M_A - M_B}{2} \\ M_{II} &= \frac{M_A + M_B}{2} \end{aligned} \qquad \text{(A16)}$$

These moments are then used in to calculate the mode I and mode II strain energy release rates. The shear corrections to G involve the mode I and mode II loading which are comparable to the applied loading of a DCB test and an ENF test, respectively.

$$(G_I)_{nl} = \frac{M_I^2}{bE_{11}I}\left(1+\frac{2}{\lambda a}+\frac{1}{(\lambda a)^2}\right)+\frac{6(P_I)^2}{5b^2G_{12}h}$$
$$(G_{II})_{nl} = \frac{3M_{II}^2}{4bE_{11}I}+\frac{9(P_{II})^2}{80b^2G_{12}h} \qquad \text{(A17)}$$

Redesigned MMB Apparatus

The nonlinear analysis of the MMB apparatus after its redesign is performed in the same manner as before. However, the location of point F and applied load are different. Because the roller is now attached to the lever, it moves with the lever and the location of the applied load is given by

$$X^F = X^A-(L+c)\cos\theta_L-(V-h-h^*)\sin\theta_L$$
$$Y^F = Y^A-(L+c)\sin\theta_L+(V-h-h^*)\cos\theta_L \qquad \text{(A18)}$$

Since the roller bears on a horizontal surface attached to the load frame, the applied load remains vertical.

$$P_Y^F = -P_a$$
$$P_X^F = 0 \qquad \text{(A19)}$$

Therefore to analyze the redesigned apparatus, equations A18 and A19 are substituted for equations A8 and A10, respectively.

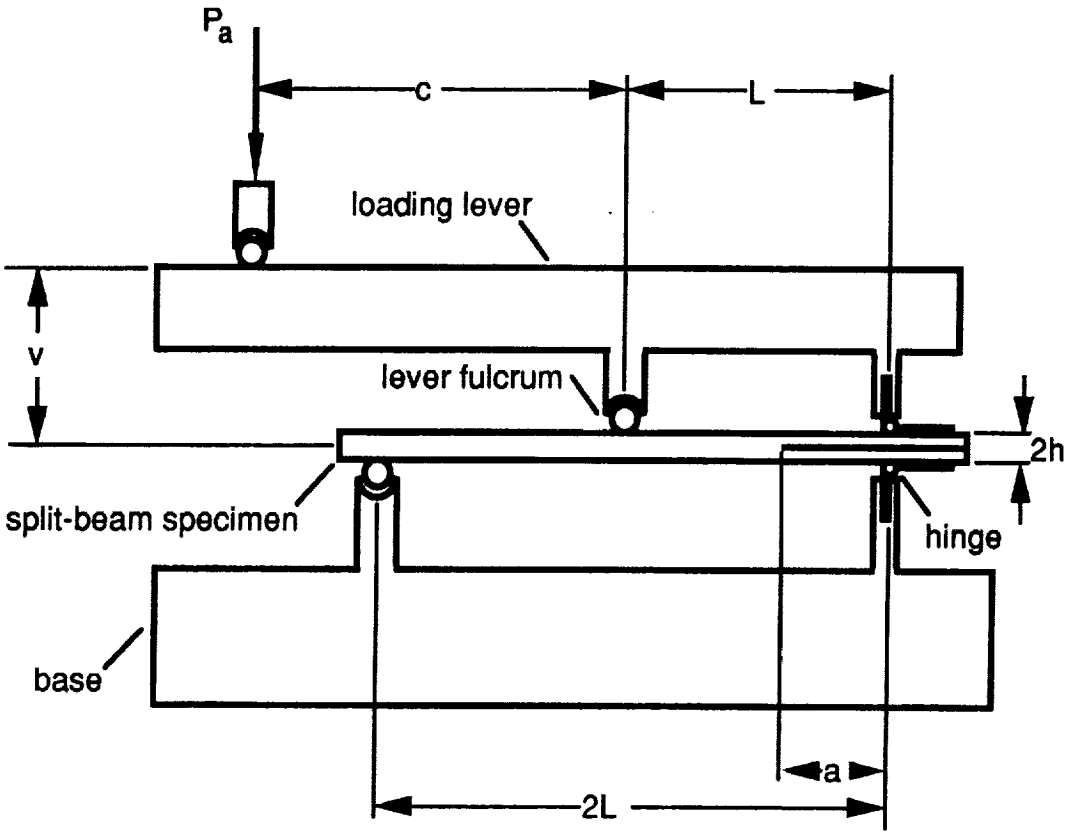

(a) Undeformed position.

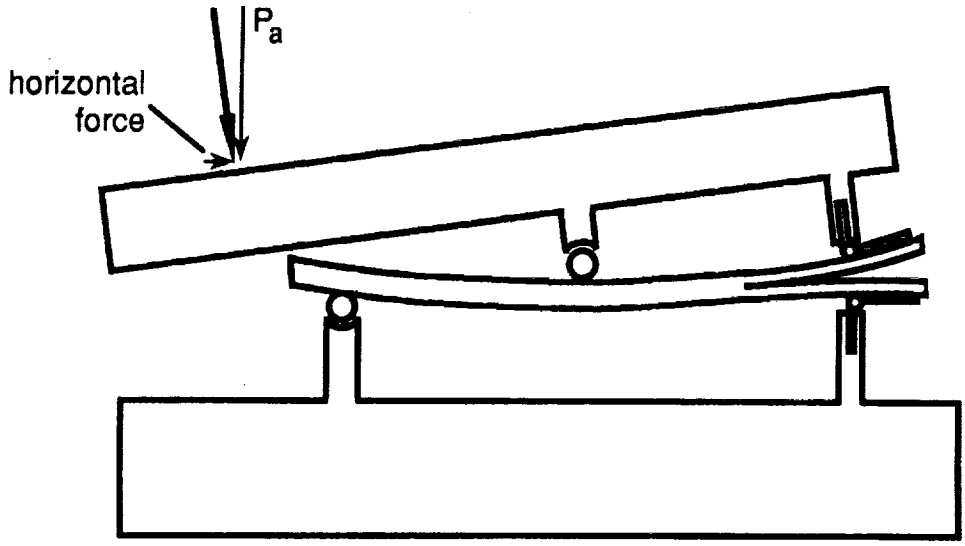

(b) Deformed position.

Figure 1.- Original mixed-mode bending test apparatus.

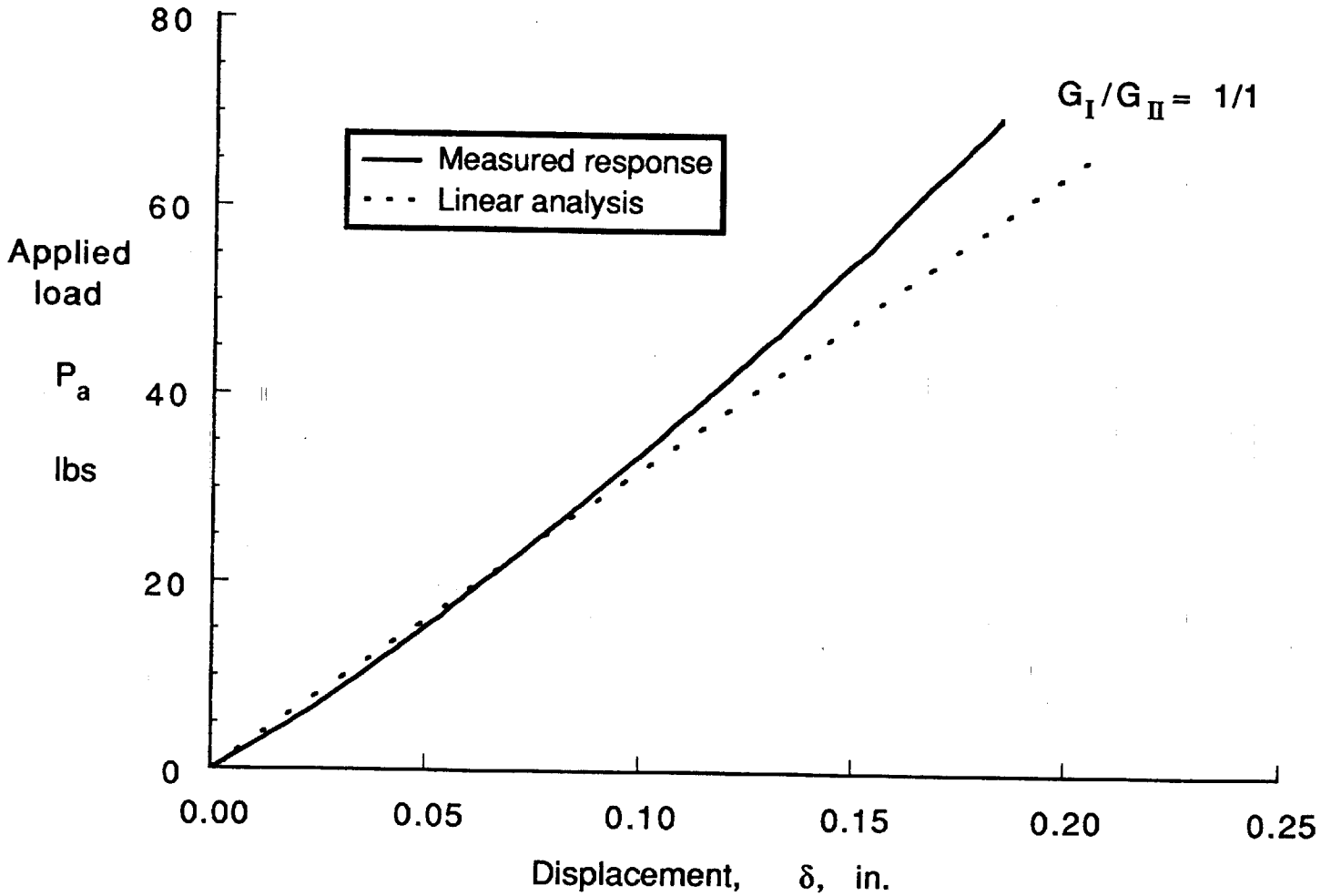

Figure 2.- Nonlinear response of an APC2 split beam specimen in the original MMB apparatus.

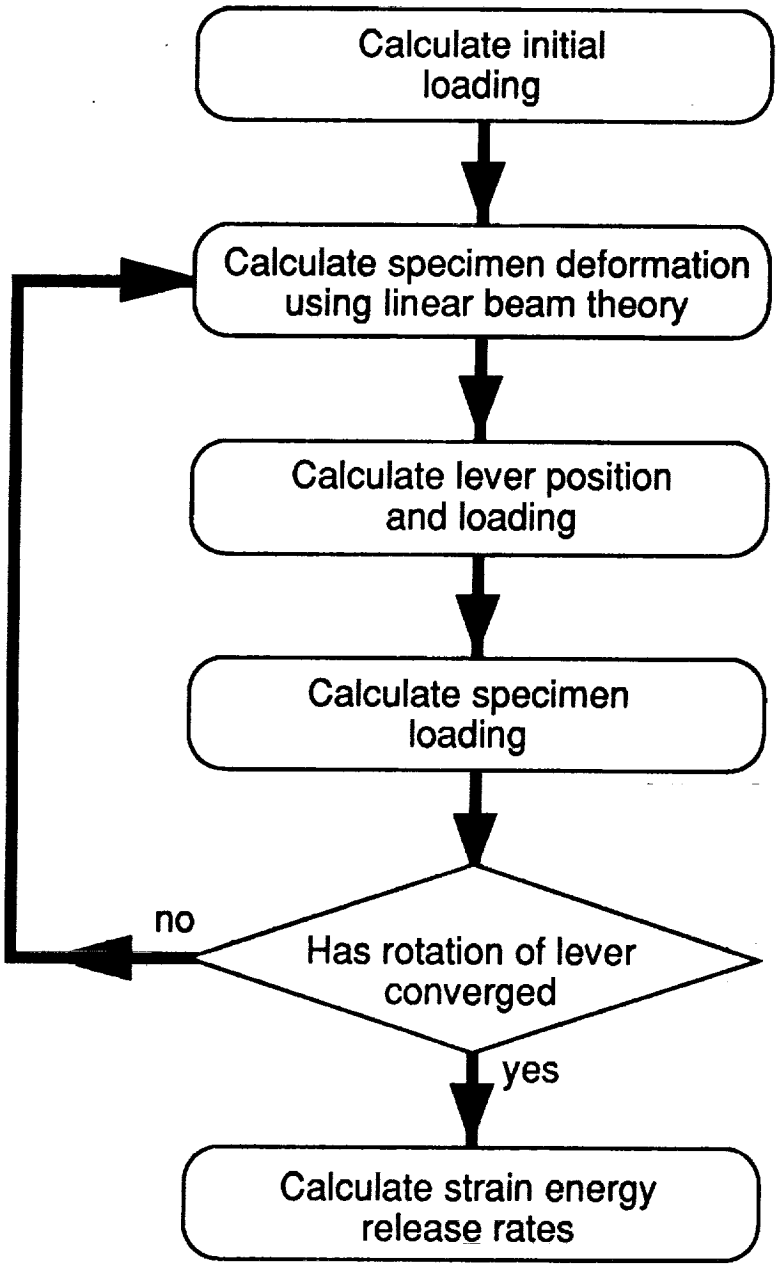

Figure 3.- Flow diagram for nonlinear analysis of mixed-mode bending test.

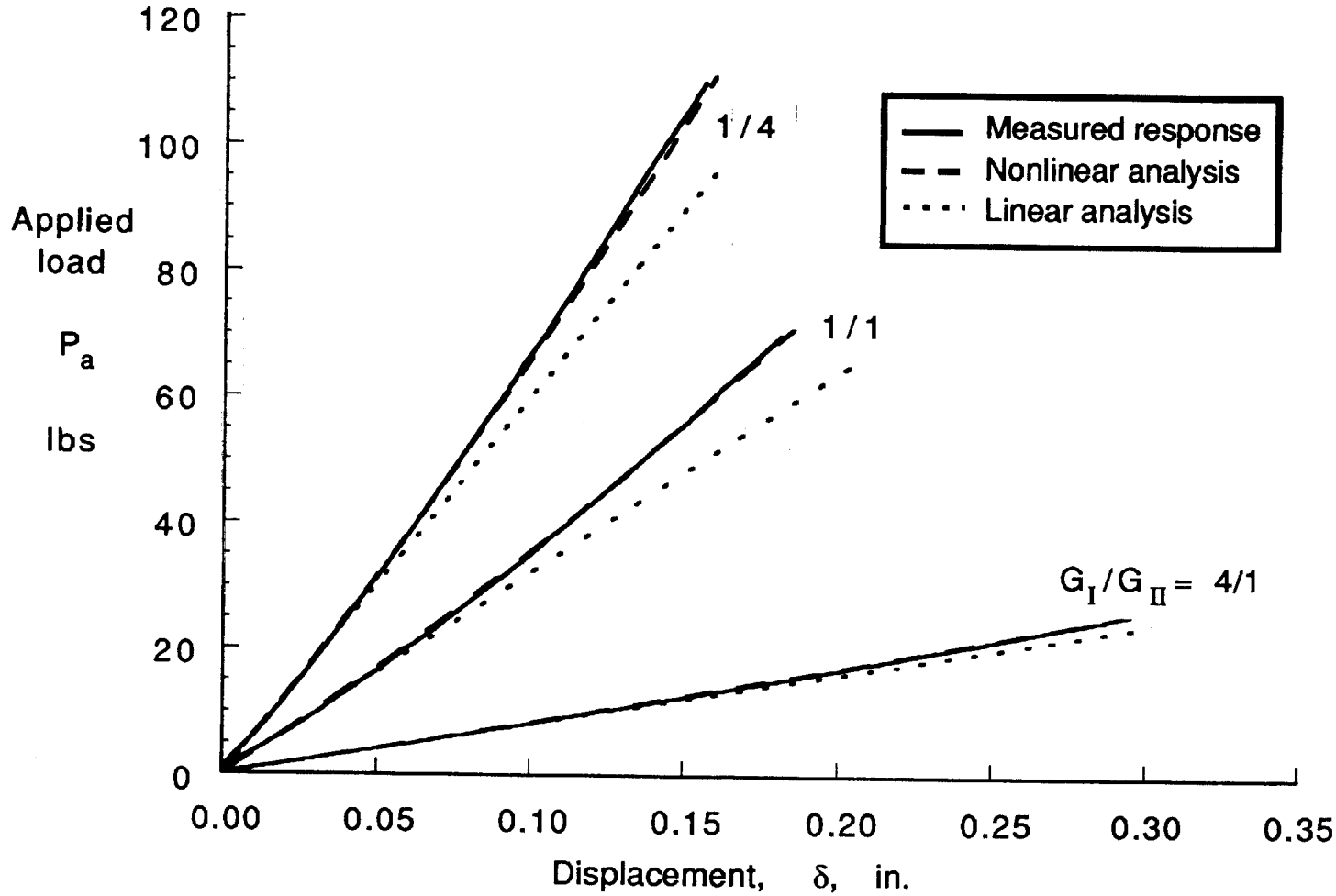

Figure 4.- Measured and calculated load-displacement curves of an APC2 split beam specimen in the original MMB test apparatus.

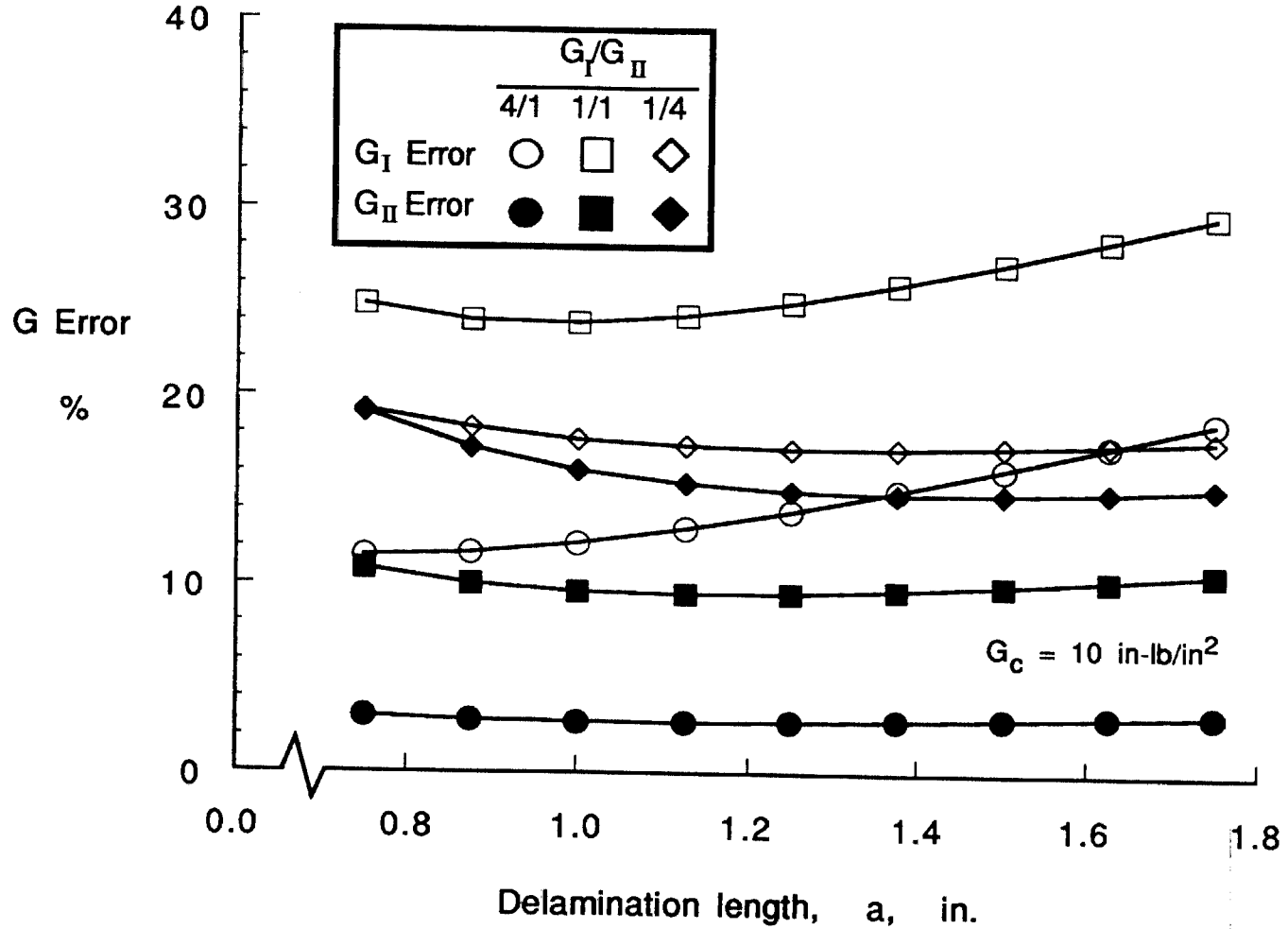

Figure 5.- Error due to nonlinearity of MMB test.

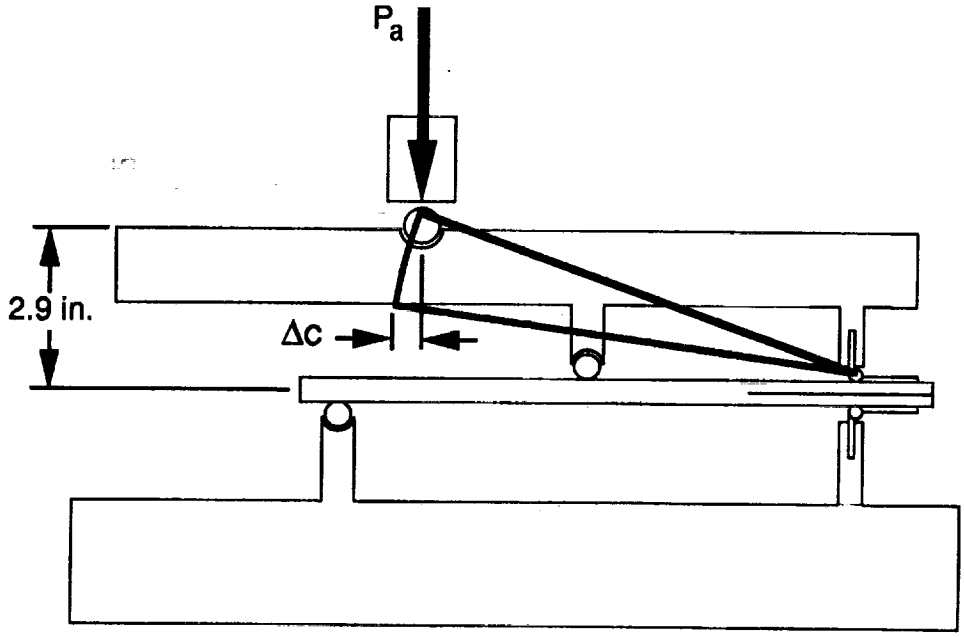

(a) Original lever height.

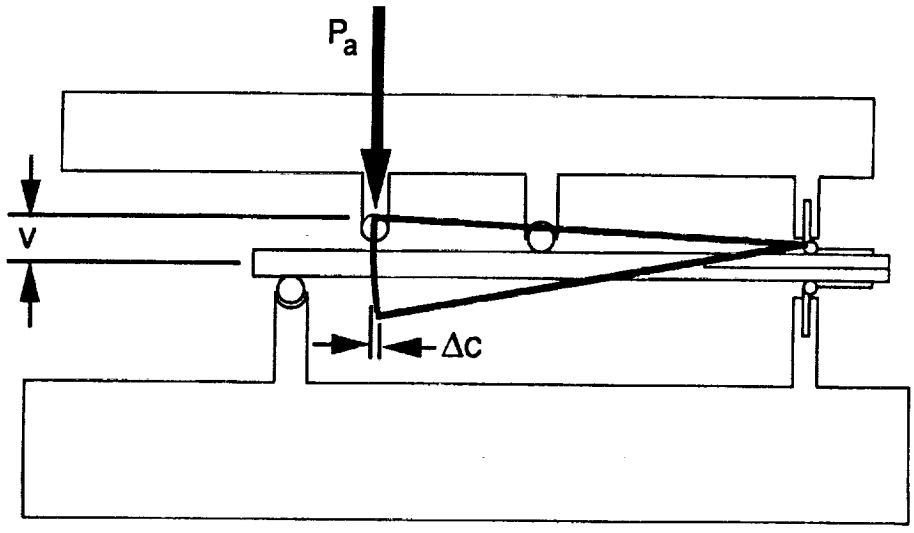

(b) Lower lever height.

Figure 6.- Effect of lever height on load point translation.

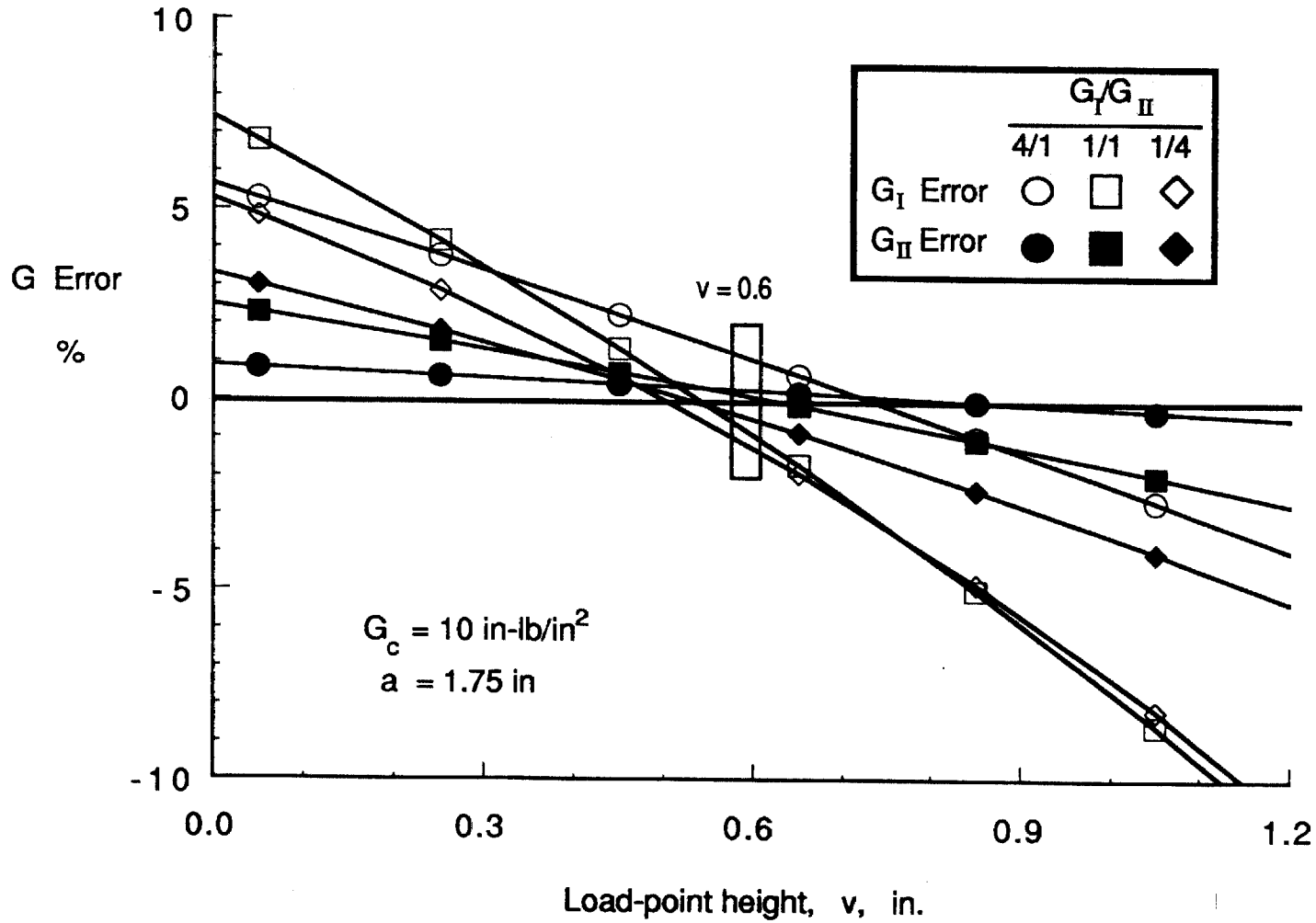

Figure 7.- Effect of load-point height above specimen mid-plane on G error.

ORIGINAL PAGE
BLACK AND WHITE PHOTOGRAPH

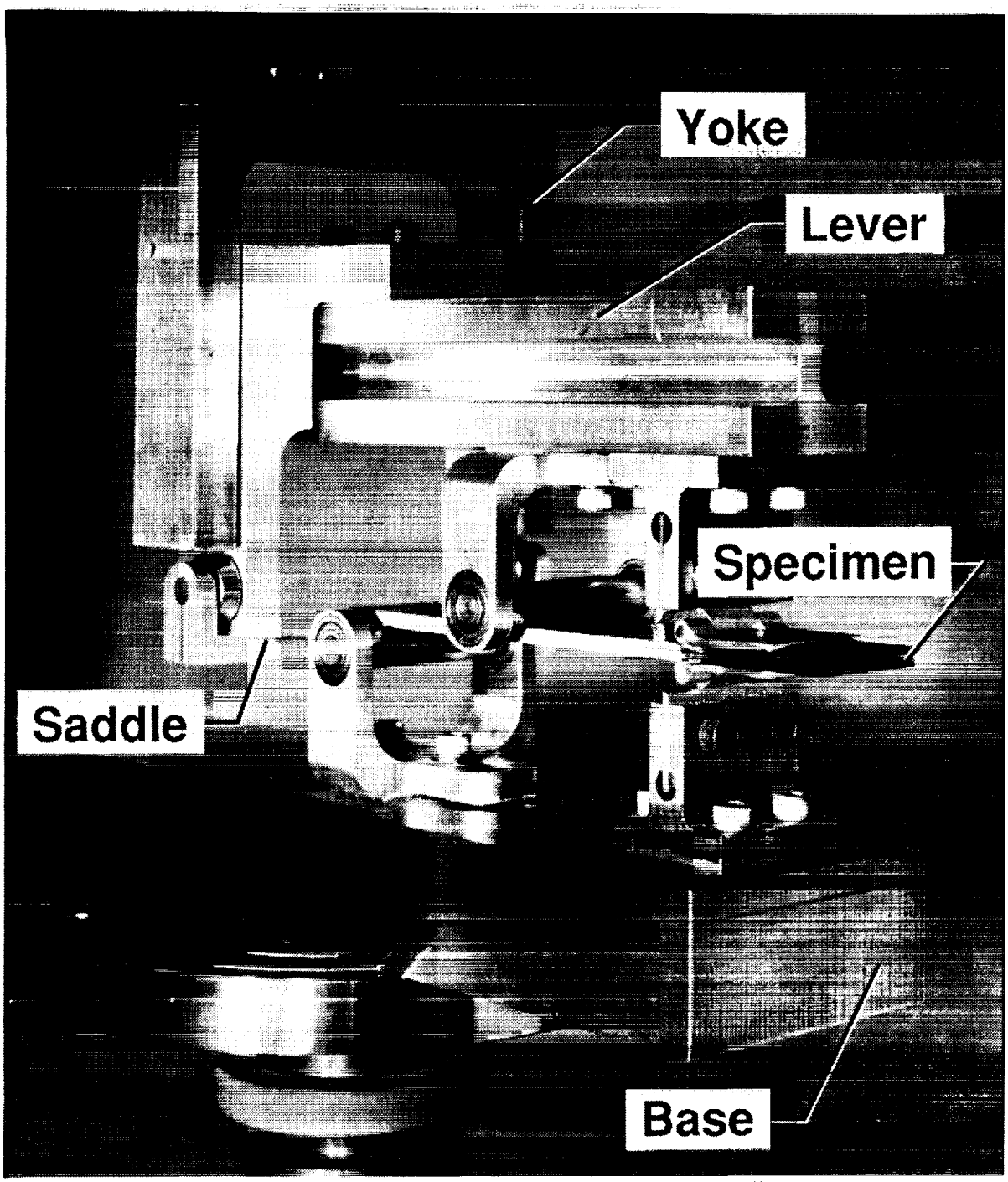

Figure 8.- Redesigned MMB apparatus

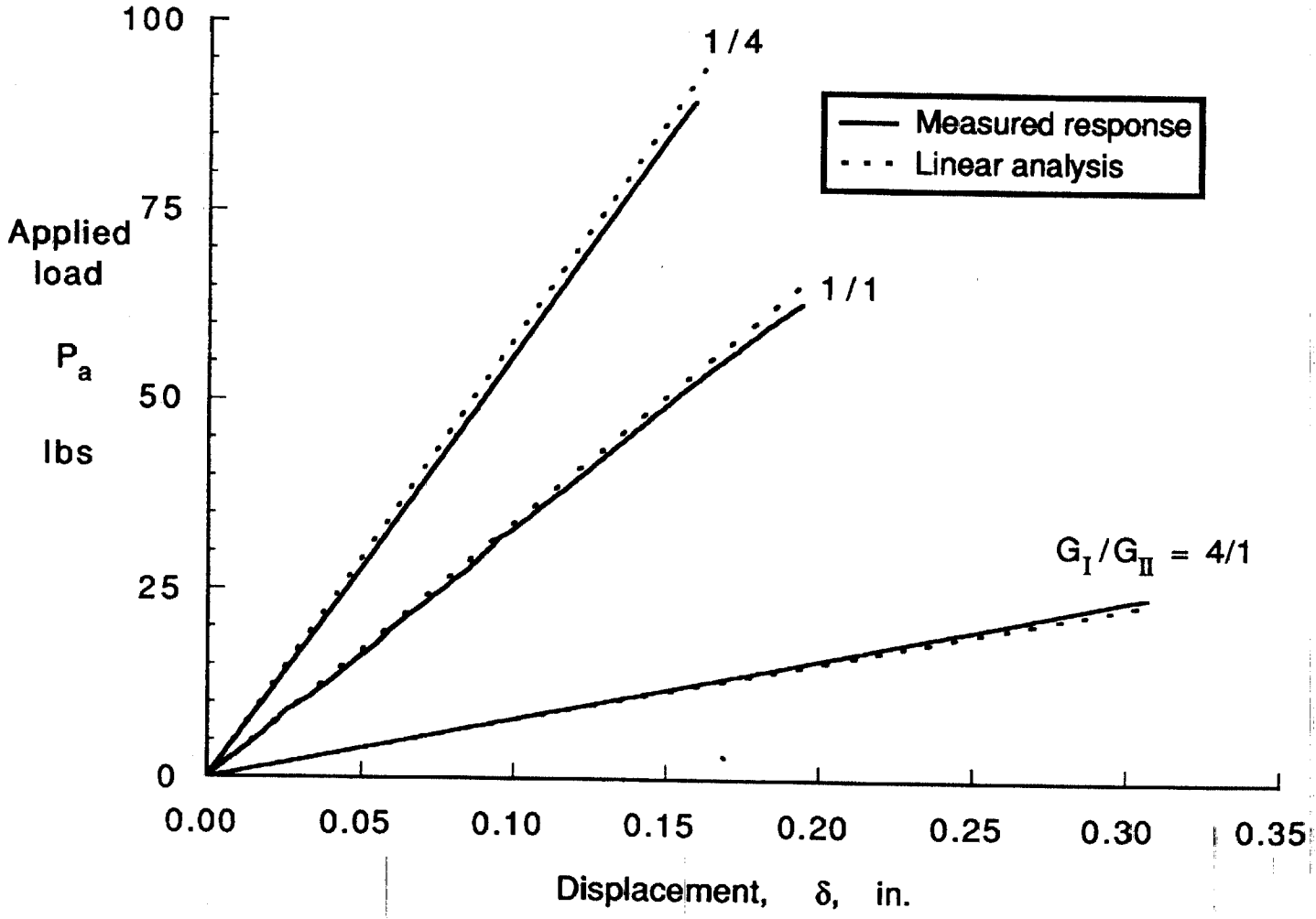

Figure 9.- Load-point displacement response of an APC2 split beam specimen in the redesigned MMB apparatus.

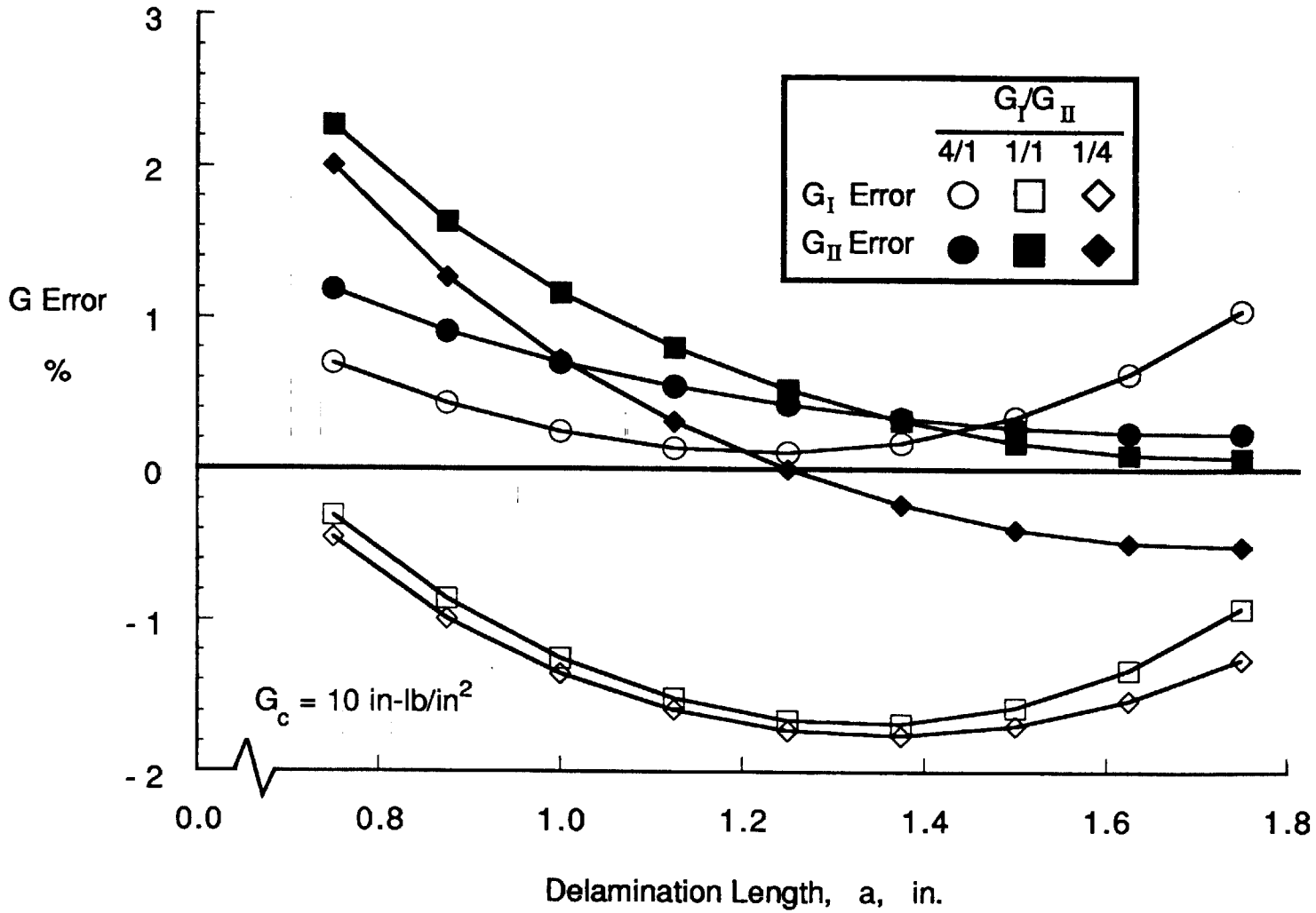

Figure 10.- Error in G calculation for the redesigned MMB test.

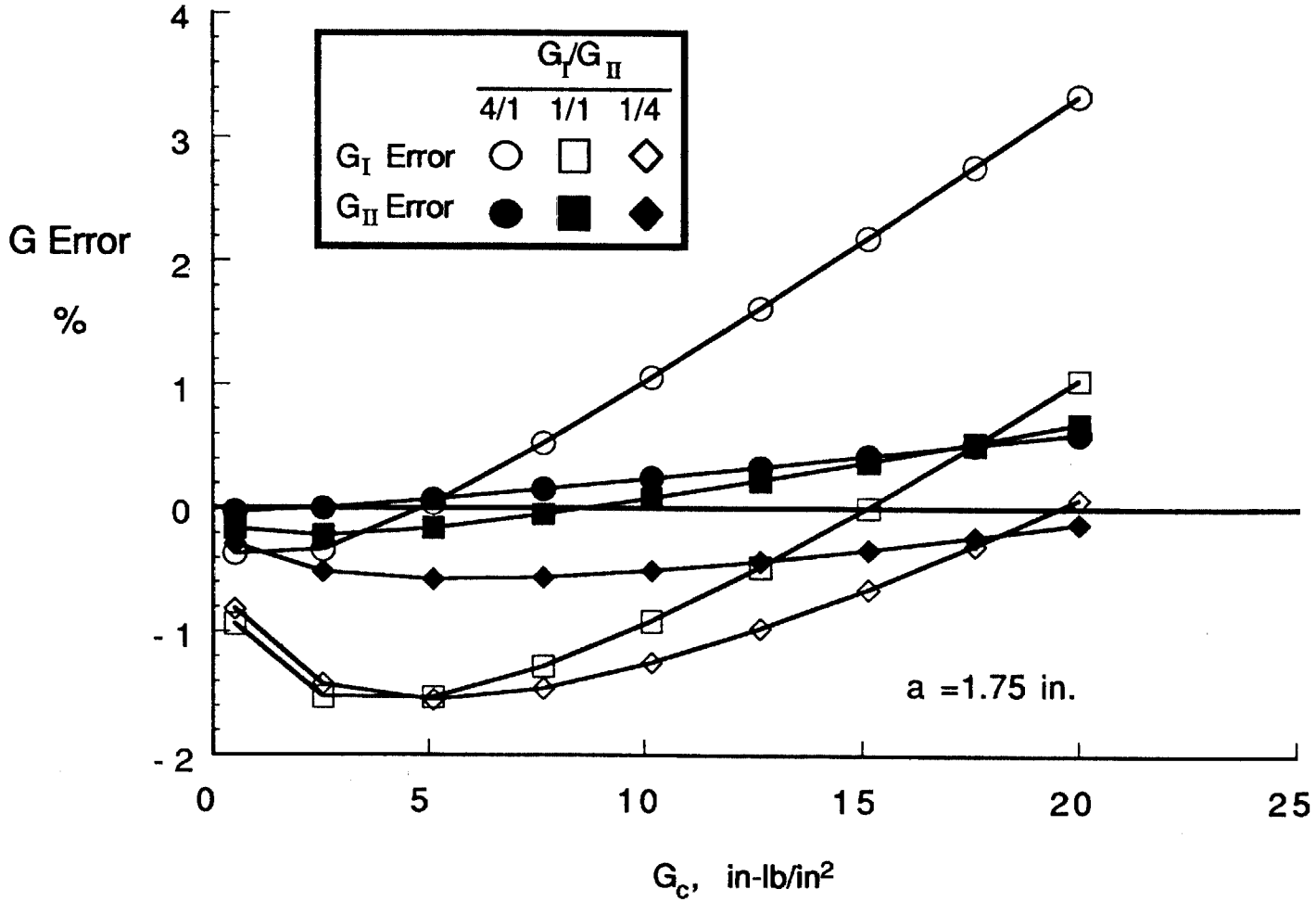

Figure 11.- Error in G calculation for varying material toughness.

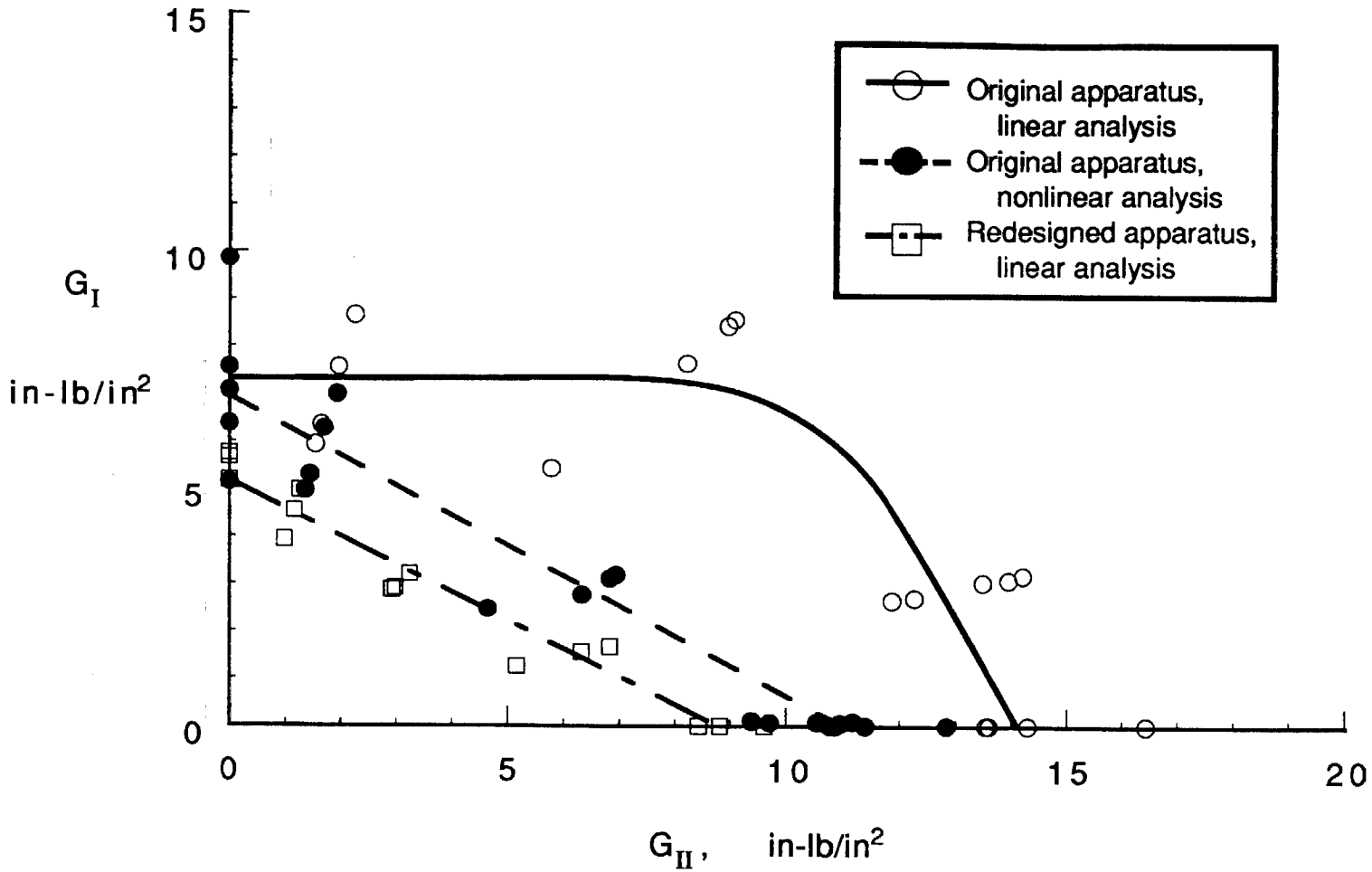

Figure 12.- Mixed-mode interlaminar fracture toughness of APC2 with 4/1 mixed mode ratio precrack.

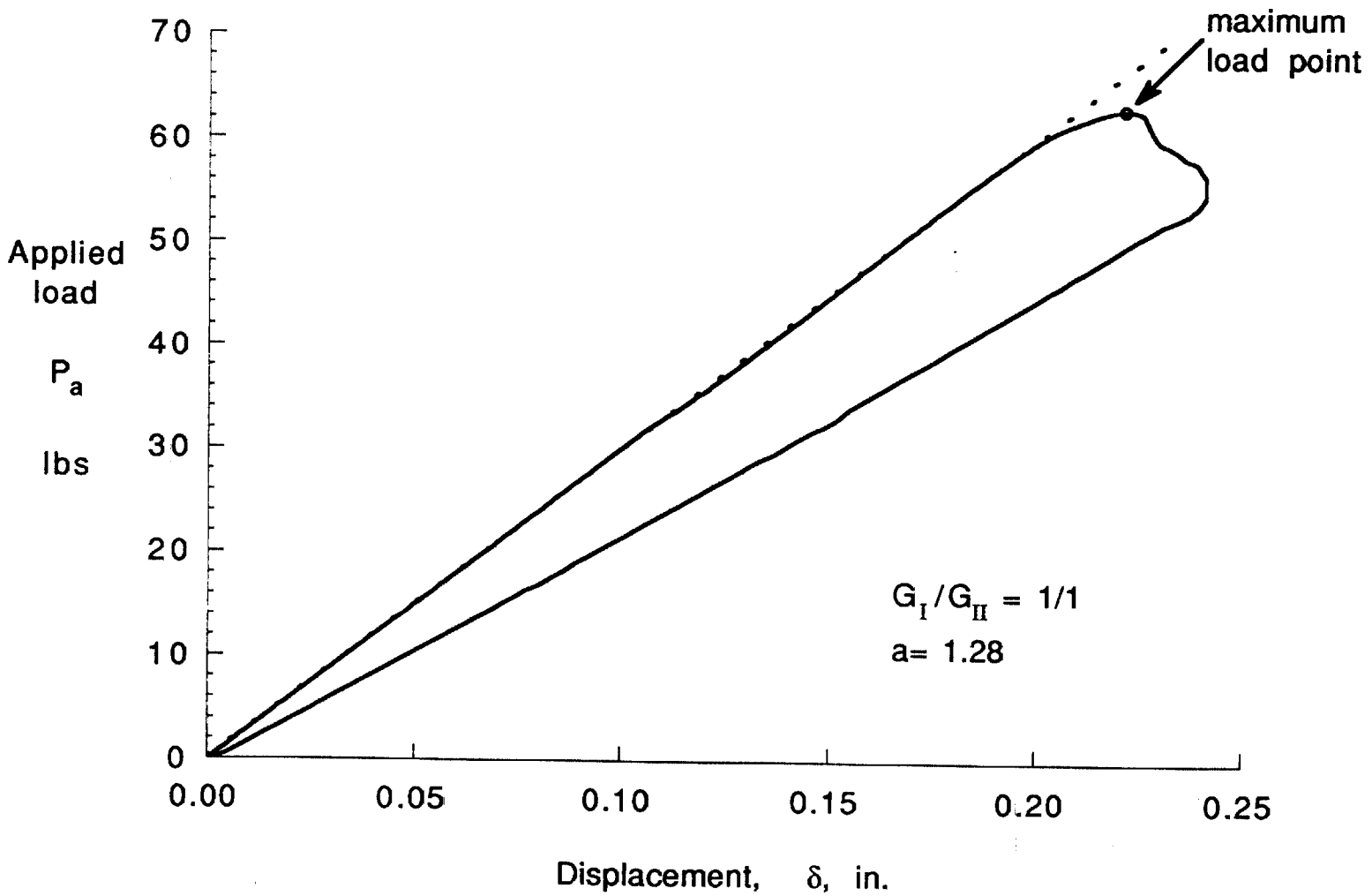

Figure 13.- Typical load displacement curve for the redesigned MMB test.

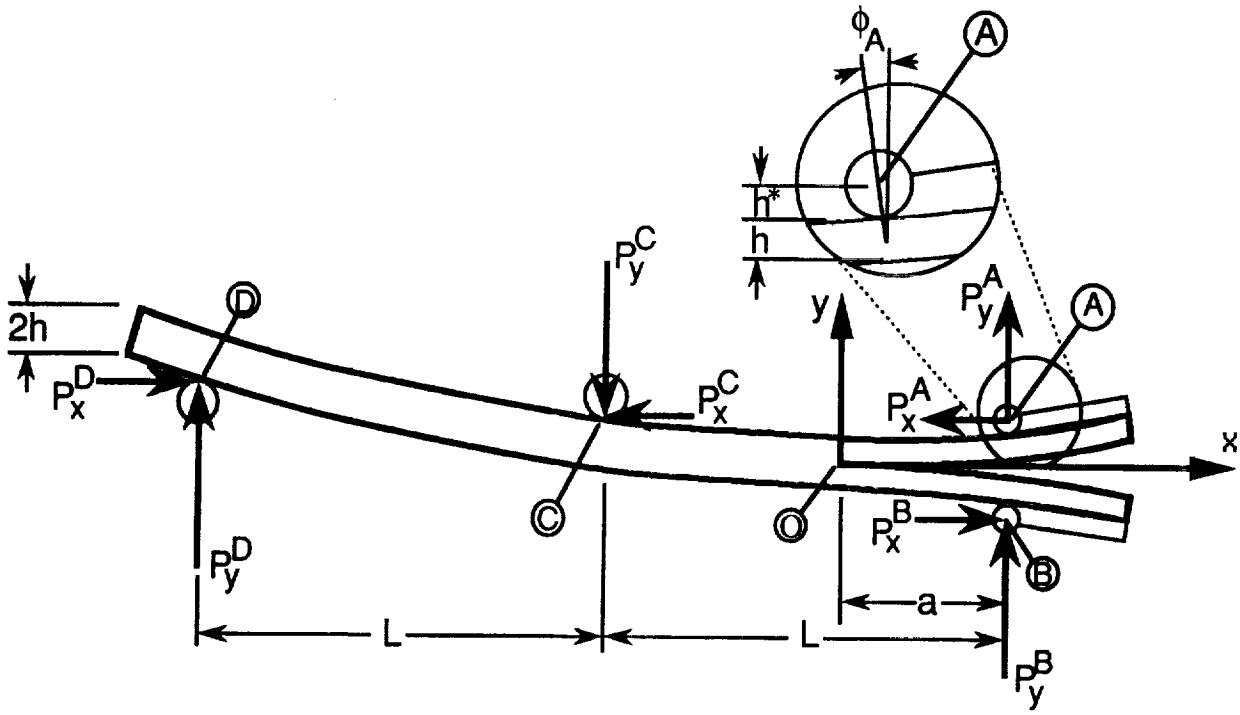

(a) Specimen geometry.

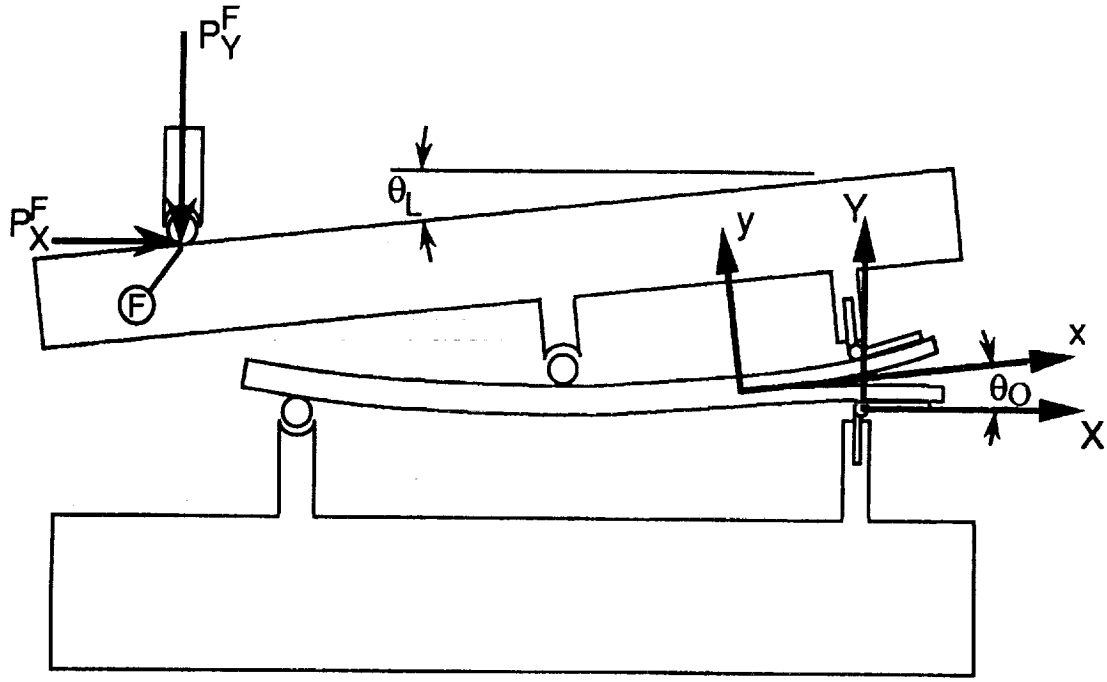

(b) Apparatus geometry.

Figure A1.- Notations used in nonlinear analysis.

NASA National Aeronautics and Space Administration

Report Documentation Page

1. Report No.	2. Government Accession No.	3. Recipient's Catalog No.
NASA TM-102777		

4. Title and Subtitle	5. Report Date
Nonlinear Analysis and Redesign of the Mixed-Mode Bending Delamination Test	January 1991
	6. Performing Organization Code

7. Author(s)	8. Performing Organization Report No.
J. R. Reeder and J. H. Crews, Jr.	
	10. Work Unit No. 505-63-01-05

9. Performing Organization Name and Address	11. Contract or Grant No.
NASA Langley Research Center Hampton, VA 23665-5225	
	13. Type of Report and Period Covered Technical Memorandum

12. Sponsoring Agency Name and Address	14. Sponsoring Agency Code
National Aeronautics and Space Administration Washington, DC 20546-0001	

15. Supplementary Notes

16. Abstract

The Mixed-Mode Bending (MMB) test uses a lever to simultaneously apply mode I and mode II loading to a split-beam specimen. An iterative analysis that accounts for the geometric nonlinearity of the MMB test was developed. The analysis accurately predicted the measured load-displacement response and the strain energy release rate, G, of an MMB test specimen made of APC2 (AS4/PEEK). The errors in G when calculated using linear theory were found to be as large as thirty percent in some cases. Because it would be inconvenient to use a nonlinear analysis to analyze MMB data, the MMB apparatus was redesigned to minimize the nonlinearity. The nonlinear analysis was used as a guide in redesigning the MMB apparatus. With the redesigned apparatus, loads are applied through a roller attached to the level and loaded just above the midplane of the test specimen. The redesigned MMB apparatus has geometric nonlinearity errors of less than three percent, even for materials substantially tougher than APC2. This apparatus was demonstrated by measuring the mixed-mode delamination fracture toughness of APC2. The data from the redesigned MMB apparatus were analyzed with a linear analysis which yielded results similar to those found with the original apparatus and the nonlinear analysis.

17. Key Words (Suggested by Author(s))	18. Distribution Statement
Mixed-mode delamination Composite Nonlinear analysis Toughness testing Graphite/PEEK	Unclassified - Unlimited Subject Category - 39

19. Security Classif. (of this report)	20. Security Classif. (of this page)	21. No. of pages	22. Price
Unclassified	Unclassified	42	A03